2024 IEEE/RSJ International Conference on Intelligent Robots and Systems (IROS)
October 14-18, 2024. Abu Dhabi, UAE

State Estimation of an Adaptive 3-Finger Gripper using Recurrent Neural Networks

Yannick Jonetzko, Theresa Alexandra Aurelia Naß, Niklas Fiedler, and Jianwei Zhang[1]

***Abstract*— Adaptive grippers enable easy and robust grasping of diverse objects by adapting to their shapes and enclosing them. However, determining the exact state of the hand remains challenging. This is not always straightforward but is often necessary to assess grip success, quality, or the pose of the object. In this work, we present two deep learning approaches using recurrent neural networks to successfully estimate the joint states of the Robotiq 3-Finger Adaptive Gripper. The models are compared with an existing analytical approach, which does not distinguish between the fingers of the hand and calculates the three angles of their respective joints using joint limits, contact information, and motor position in a transition model. We test the differences in accuracy with our networks by not distinguishing between the fingers as the analytical approach for the first model and by looking at the entire hand in the second model. Our experiments demonstrate that the model considering the entire hand outperforms the other two approaches, is more robust against object movements and achieves an average joint position accuracy of 2.29 degrees.**

I. Introduction

Accurate grasping and the ability to predict and evaluate grasps are significant challenges in robotics, particularly in tasks where robots interact with objects in unstructured environments. Without knowing whether or how an object has been grasped, manipulating it becomes exceedingly challenging, if not risky. There is a potential for unintended movement, tipping, or even damage to the object. In an ideal scenario, precise knowledge of the spatial arrangement of the robot and the environment would be required. Realistically, achieving such precision is not possible or requires excessive effort. Robotic hands like the Shadow Hand, which can consistently maintain and control their state precisely, are complex, fragile, costly, and challenging to operate. In contrast, underactuated and soft grippers like the qb SoftHand Research offer a simpler user experience and adapt automatically to objects, easing the process of successful grasping [1, 2]. However, they lack the capability to precisely determine the exact state of the hand, posing difficulties for precise manipulation and interaction. Utilizing more sensors and modalities provides a closer approximation of the robot and the environment and facilitates the interaction of robots.

In the present work, we introduce a novel approach to determine the current state of the underactuated 3-Finger Gripper from Robotiq using contact sensors and deep learning. Franchi and Hauser [3] presents a way to determine the state of this gripper analytically way and simulate the behavior of the gripper. The premise of this work is based on the assumption that objects do not move when touched or when forces are exerted on them from multiple directions by the fingers. However, errors can occur in the calculated state if the object moves and changes a contact point, as the calculation relies on the previous joint states of a finger. Furthermore, only closing motions are estimated since the opening can be neglected. We take this paper as state-of-the-art for Robotiq's gripper and compare it with our deep learning approaches. The main contributions of our work are:

- We implemented a robust joint state estimation of the underactuated Robotiq 3-Finger Adaptive Robot Gripper utilizing contact data.
- The estimation is more robust against object movement than the existing analytical approach.

The remainder of the paper is structured as follows: Section II presents related work to the paper at hand. In Section III, we present the robot gripper, our custom-built contact sensors, and the visual tracking setup. In Section IV, we describe our approach and the architecture of our neural network. Section V presents our experiments and data collection, followed by the results and discussion in Section VI and Section VII. In Section VIII, we conclude the paper and give an outlook to potential future work.

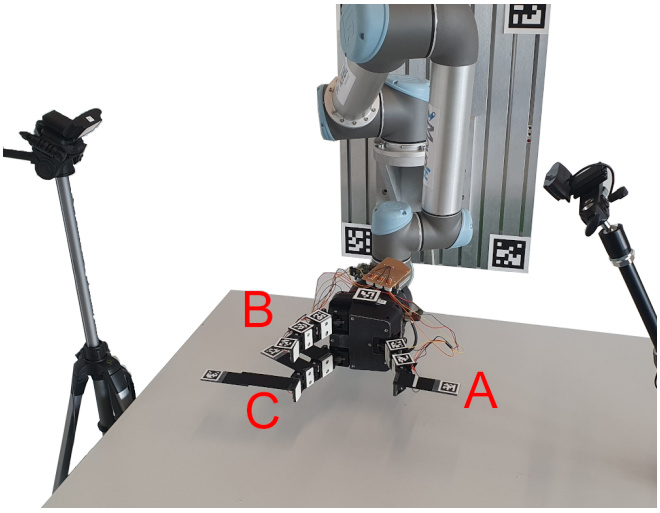

Fig. 1. The underactuated Robotiq 3-Finger Adaptive Robot Gripper with custom-built contact sensors and an AprilTag tracking setup to detect ground truth data. Two cameras observe the tags from the side of the gripper at an angle.

*This research was funded by the German Research Foundation (DFG) and the National Science Foundation of China in the project Crossmodal Learning, TRR-169.

[1]is with group Technical Aspects of Multimodal Systems (TAMS), Department of Informatics, Universität Hamburg, Germany yannick.jonetzko@uni-hamburg.de

II. Related Work

The closest work is the publication by Franchi and Hauser [3], where the same gripper is used and the joint state of the hand is determined using contact information and mathematical calculations. This model is used to simulate the gripper in Klampt. However, this approach only partially works on the real robot, as it assumes a rigid world without considering object dynamics. The extent to which the results differ from our paper is discussed in Section VII. Another work that calculates underactuated fingers using kinematic analysis is done by Meng et al. [4].

In [5], the authors learn a state transition model of their underactuated gripper with the position of the object, actuators angles, and actuators loads as input. With their two-finger gripper with two joints each, trajectories of manipulation motions are recorded to determine the joint state.

Using an underactuated gripper with Reinforcement Learning (RL) enables the robot to manipulate objects without needing kinematic models or analytic dynamics. However, the current joint state of the gripper is not known. Van Hoof et al. [6] use tactile features to learn in-hand manipulation motions with RL without models of the objects. RL could also be used to learn hard to achieve manipulation tasks like grasping shallow objects [7]. In this case, the authors also provided the gripper with a custom-built fingertip nail. Liu et al. [8] use RL to control an anthropomorphic hand by shape memory alloy.

Instead of determining the state of the gripper, it is common to estimate the pose of the grasped object directly. Azulay et al. [9] utilized haptic information in the form of kinesthetic and tactile feedback to determine the pose of a grasped object. In their setup, they employed a gripper with two underactuated fingers and used a model predictive control approach to manipulate the object in hand.

Determining the state of a soft gripper is even more complex, as the degrees of freedom are typically higher. Matsuno et al. [10] has designed a printable soft finger with air chambers that bend with increasing pressure. On the backside of this finger, electro-conductive yarn is attached, running from the base of the finger to the fingertip and back again. They built a gripper with three fingers arranged in a circle. By monitoring the resistance change of the yarn, they determine the diameter of the grasped object and can thereby estimate the bending state of the finger. Several similar works follow this approach [11, 12, 13].

Several works implement the behavior of underactuated grippers in simulation [14, 15, 16]. These approaches often rely on assumptions that do not hold in a real system, thus functioning only in simulation.

III. Hardware Setup

A. 3-Finger Adaptive Gripper

We use the 3-Finger Adaptive Gripper from the Robotiq company in our robot laboratory. The hand was designed to be robust and precise for use in both industrial applications and research purposes. Sadun et al. [17] provide a comprehensive analysis of grasping and present the technical details and grasping capabilities in more detail than we will do here.

The hand has 3 fingers, A, B, and C (see Figure 1), with B and C closing in parallel while A closes opposite between the other two. The fingers are controlled by four actuators and have 10 degrees of freedom (DoF). Finger A is controlled by one actuator and has 3 DoF. B and C share an additional actuator that spreads the fingers apart or moves them together until their fingertips touch, thus sharing an additional degree of freedom. The joint state of this shearing motion is not predicted in this work, as it can be derived directly from the motor position. The remaining three motors each close one finger and thus move three underactuated joints. In Figure 2 the range of the three joints can be seen as well as the rotary axis of the motor with g as motor position. With two torsion springs per finger and a mechanism consisting of several links behind the phalanges, an adaptive finger behavior and adaptation to objects is produced. By changing the motor position of the fourth actuator between fingers B and C, the hand can be moved to different grasping modes (basic, wide, pinch, and scissors). As the fingers' underactuation is independent of the grasping mode, we will only examine the basic mode in this work. The position of the motors, g, is differentiated into 255 values, with the actual range of motion between 6 (fully open) and 240 (fully closed). The hand provides several measurements, including the position of each motor, a value representing instantaneous current consumption, and an object detection value. Previous tests have shown that these values, except for the motor position, are not suitable for assessing the state.

B. Contact Sensors

The construction process of the custom-built contact sensors is described in [18]. This paper focuses on manufacturing tactile sensor arrays, however, in this scenario, the precise contact point or spatial shape of the objects is not of interest. Instead, the concern is whether contact has been

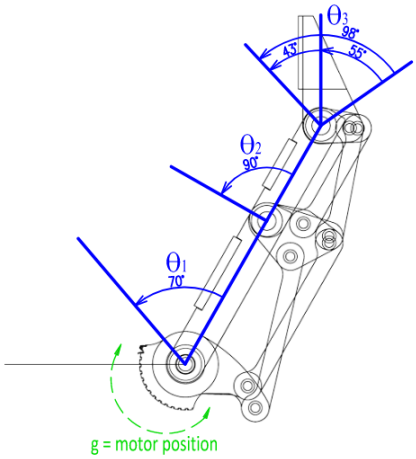

Fig. 2. The range of each joint of the grippers fingers. g represents the motor position. [3]

made and the force exerted. Therefore, only one taxel was installed per phalanx. The sensor is constructed from several layers. The bottom layer consists of aluminum adhesive tape cut to size and directly adhered to a 3D-printed adapter. On top of this layer, a slightly larger cutout velostat foil is placed, followed by a second layer of aluminum. The entire assembly is secured with transparent adhesive tape. Finally, a 1 mm thick silicone mat serves as the top layer to improve pressure distribution. The fully assembled sensors are depicted in Figure 3.

In the readout circuit, the sensor is part of a voltage divider next to a 10 kΩ resistor. A change in pressure onto the sensor results in a changed resistance. Thus, the voltage output of the divider reflects the amount of pressure. This voltage is measured by a 10 bit analog to digital converter in the microcontroller at a rate of 50 Hz. The read value is zeroed at the beginning of each grasp and normalized between 0 and 1. All sensors provide comparable and reproducible values, but in this scenario, they are not calibrated and therefore do not deliver physical force values. If a sensor touches an object and moves it, the read value is below 0.4. If forces are exerted from two sides of the object, the value increases sharply and from a value of over 0.7 we interpret this as contact in the analytical approach.

C. Visual Tracking

A visual tracking system with fiducial markers is integrated onto the gripper to generate ground truth training and validation data. AprilTags [19] are attached together with the contact sensors to custom 3D-printed parts, which replace the distal, medial, and proximal phalanx pad (see Figure 3). An additional tag is attached to the palm of the hand. The markers are observed using two calibrated conventional webcams with 30 Hz from a distance of 50 cm, angled from the side to minimize occlusion. This setup ensures that at least two fingers are always visible. The z-axes of the tags all point in the same direction, allowing the angle between two tags to be calculated from their respective x-axes or y-axes. With this approach we can determine the angles between two joints to an accuracy of half a degree.

IV. Approach

The aim of this work is to always know an estimated state of each fingers three joints. As the only available measurement is the motor position of one motor per finger, it is not possible to directly infer the joint positions from this measurement alone. Additionally, the hand provides a measurement representing the instantaneous current consumption. However, it has proven unhelpful in state estimation as it only triggers when the hand has completed a grasp, so it is not considered further.

Visual tracking of the hand is theoretically possible, but due to constant occlusion and the need for a camera to monitor the scene constantly, this system is impractical. We implemented such a system for our ground truth tracking, depicted in Figure 1. With its protruding markers, it would not be suitable for continuous operation and only works in this fixed setup.

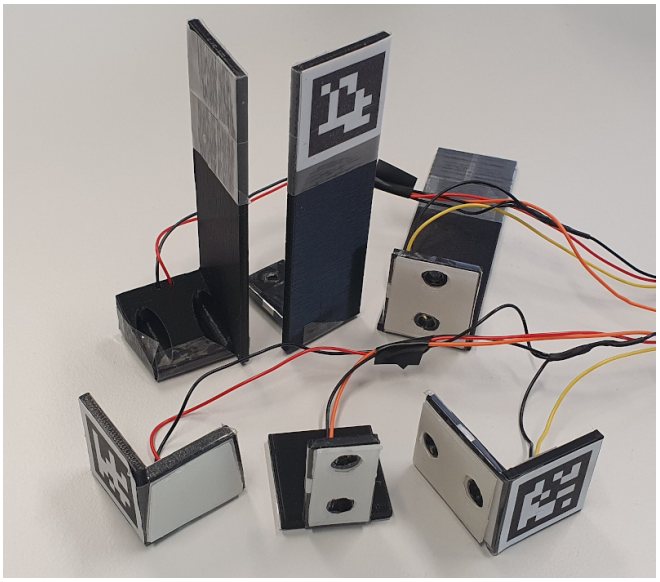

Fig. 3. Contact sensors and fiducial marker tracking system integrated into custom 3D-printed fingertip, medial, and proximal pads.

The problem could also be solved with additional joint encoders or inertial measurement units (IMUs), with which the joint position can be read out directly. However, this would entail a considerable hardware change which may not justify the effort involved.

An alternative approach, commonly used in the state of the art and thus used in this work, is the use of contact sensors on all phalanges. They are easy to integrate and provide data on contacts with the object, enabling the calculation of finger states. Compared to encoders or IMUs, contact sensors are often already present on grippers and do not have to be integrated separately. Thus, we have four measurement points per finger: one motor position and three contact values. Since these four measurement points do not directly determine the joint angles, another factor must be considered: the progression over time or the previous condition of the hand.

With this information, Franchi and Hauser [3] shows that it is possible to calculate the angles mathematical, but only under the premise that the object being grasped does not move. In this work, we implement an approach using recurrent neural networks to determine finger behavior even under the movement of objects. We subsequently compare the results with Franchi and Hausers analytical approach.

A. Analytical Approach

Franchi and Hauser [3] have shown that it is possible to create a mathematical model of the states of Robotiq's three-finger hand. The resulting kinematic model is used and validated in simulation. Shortly summarized, the relative change in the three joint angles can be calculated by dividing the closing movement into four phases (see Table I). Each phase is determined by a tuple describing whether contacts

TABLE I
ANALYTICAL JOINT STATE CALCULATION [3]

Phase	State tuples	$\Delta\Theta_1$	$\Delta\Theta_2$	$\Delta\Theta_3$	Δg
1	(0,0,0,0,0,0)	$f_1(x,u)$	0	$-f_1(x,u)$	u
1'	(0,0,0,0,0,-1)	$f_1(x,u)$	0	0	u
2	(1,0,0,0,0,0), (0,0,0,1,0,0)	0	$f_2(x,u)$	$-f_2(x,u)$	u
2'	(1,0,0,0,0,-1), (0,0,0,1,0,-1)	0	$f_2(x,u)$	0	u
3	(·,1,0,·,0,0), (·,0,0,·,1,0)	0	0	$f_3(x,u)$	u
4	(·,·,1,·,·,0), (·,·,0,·,·,1)	0	0	0	u

or joint limits are present ($c_1, c_2, c_3, l_1, l_2, l_3$). A value of 1 means that the joint is either in contact or at a limit. -1 is the opening limit of joint 3, and · means that either c_i or l_i is 1. The relative changes are added to the previous joint state. In the first phase (1,1'), the fingers close without a contact or limit, in phase two (2,2') the proximal phalanx is either in contact or limit. In phase three (3), the middle phalanx is in contact or limit independent of the state of the proximal one and in the last phase (4), the fingertip is in contact or limit independent of both the proximal and middle phalanx. And therefore, the grasp finished when phase four occurs The joint changes are calculated using the following equations:

$$f_1(x,u) = m_1 * u, \text{ with } m_1 = \frac{\Theta_{1,max}}{140}$$
$$f_2(x,u) = m_2 * u, \text{ with } m_2 = \frac{\Theta_{2,max}}{100}$$
$$f_3(x,u) = m_3(g) * u,$$
$$\text{with } m_3(g) = \Theta_{3,min} + \frac{\Theta_{3,max} - \Theta_{3,min}}{255 - g}$$

With $u \in [-1, 1]$ describing the change in g from one time step to the next.

B. Recurrent Neural Network Approach

The state of the hand cannot be determined at any arbitrary point in time because it is always necessary to know the previous state, at least from the moment the first contact occurred and the fingers started to adapt. Recurrent neural networks (RNNs) are neural network architectures specifically designed for such sequential information. They excel at capturing information and dependencies over time or sequences. In our case the time or state value is the motor position g. In this work we use the most common RNN Long short-term memory (LSTM) [20], as it shows suitable for this task and outperformed Gated Recurrent Units (GRU) in our experiment.

1) Equal Finger Network: For this network, we do not differentiate between the fingers, i.e. we train a network that receives information from three contact sensors as a continuous value normalized between 0 and 1, and a motor position value as input and outputs three joint values. Hereby we want to mimic the behavior of the analytical approach to see if an RNN approach performs better. The network consists of one LSTM layer with 148 neurons with a hyperbolic tangent (tanh) activation function. The network was trained for 1000 epochs with an adam optimizer, a learning rate of 0.002 and a weight decay of 0.00001.

2) Entire Hand Network: This network receives all nine contact information and the three motor values as input and outputs all nine joint values. The network should therefore also learn the influences of the other two fingers. Our network for the entire hand consists of an LSTM layer with 37 neurons and a tanh activation function, followed by a linear layer with 184 neurons and a Rectified Linear Unit (ReLU) activation function. We trained the network for 1000 epochs with an adam optimizer, a learning rate of 0.0009 and a weight decay of 0.00002.

The number of layers and neurons, as well as the learning rate and weight decay were determined through hyperparameter tuning.

V. EXPERIMENTS

To evaluate the accuracy of the state estimation approaches and compare them, we conducted an experiment and want to answer the following research questions:

1) Can a newly designed recurrent neural network approach outperform the existing analytical one for state estimation and compensate object movements?
2) Does an approach that takes all fingers into account at the same time perform better than not differentiating between the fingers?

To obtain the most accurate data possible, we established a fixed setup as depicted in Figure 1, with the gripper positioned approximately 15 cm above a table, oriented to grasp objects from the side. The robotic arm maintains

Fig. 4. The object set used for training, testing, and evaluating the approaches. It comprises 20 differently shaped objects of various sizes and strengths, partly from the YCB object set [21]. Each object was grasped three times.

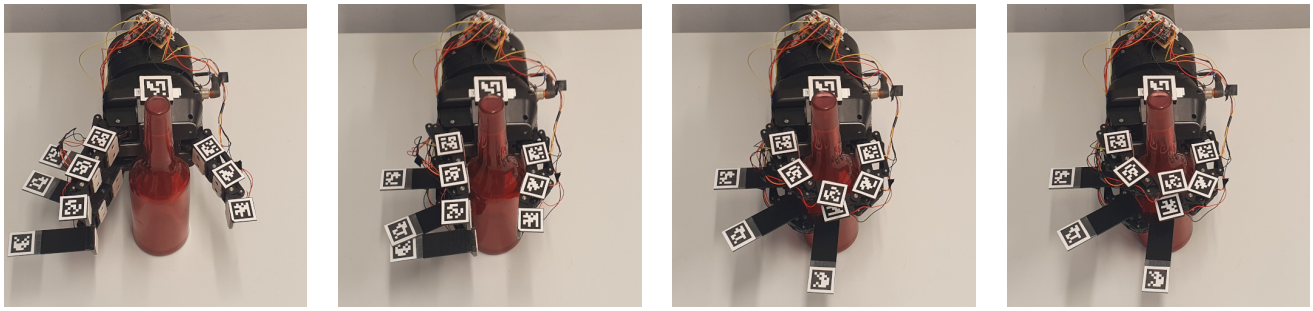

Fig. 5. An exemplary grasp with the Robotiq gripper, where the fingers adaptively conform to the object and enclose it. The AprilTags are tracked by two cameras and provide ground truth values of the joint states.

this position throughout the experiment while objects are manually positioned for the robot to grasp. Two cameras are positioned beside the gripper to optimally track the tags and minimize occlusions.

Twenty objects are grasped multiple times in different configurations to generate sample data. The object set is shown in Figure 4 and includes various everyday items such as bottles, books, tools, and similar objects with different shapes, sizes, and stiffness.

As all approaches are state-dependent, it is necessary to record data sequences. A sequence consists of exactly one finger and always starts in the fully open state. The fingers are slowly closed to capture the ground truth as accurately as possible. Since the state depends only on the previous state and not on time, it does not matter how fast we close the gripper. A sequence ends when none of the fingers are moving, indicating either a collision or reaching a limit. If a finger becomes partially occluded during the movement, the sequence for that finger is terminated from the point of occlusion. Thus, a single data point contains the contact information of the three sensors, one motor position, and the ground truth values of the tag detection.

An exemplary grasp is depicted in Figure 5, where the fingers close slowly and adaptively wrap around the object. Since the fingers make contact with the object at different times, it sometimes happens that the object is shifted. Once all fingers have made contact, the object may shift again because the two fingers on one side exert more force on the object than the opposing finger. Even if all fingers theoretically close equally, it is unlikely that we can consider each finger equally. Instead, considering all fingers together might compensate the movement. We aim to explore these effects through this experiment and answer our research questions accordingly.

VI. Results

All three approaches were evaluated using the dataset described in Section V. The dataset was split into a training set (80 %) and a test set (20 %) for the deep learning approaches.

In Table II, the average position error of the joints as well as the overall average position error are shown for the full closing motion and the finished grasp. In Figure 6 and Figure 7 the median, 25th and 75th percentiles, and 1.5 times the interquartile range are shown. All approaches have in common that the accuracy of joint 1 between the palm and proximal phalanx is the highest, the accuracy of joint 2 between the proximal and middle phalanx is lower, and the accuracy of joint 3 between the middle phalanx and fingertip is the lowest. The overall accuracy for the analytical approach is 0.142 radians, for the RNN approach with equally considered fingers 0.089 radians, and for the RNN approach considering all fingers 0.040 radians of deviation. If we only look at the end state, the overall position error of the analytical approach is 0.248 radians; for the equal finger network, it is 0.133 radians; and for the entire hand, it is 0.079 radians.

When considering the deviation trend over the values of g, representing the closure of the fingers as depicted in Figure 8, it becomes evident that the accuracy decreases as the fingers close further. In the analytical method, the error steadily increases, whereas in the LSTM methods, the error remains low for a longer duration before rising towards the end.

In Figure 9, the progression of a sample grasp of the wooden block is depicted. In the upper plots, the ground truth joint state is represented by a solid line, the trajectory of the joints from the neural network of the entire hand is indicated by a dashed line, and the analytical prediction is shown with dotted lines. The lower graphs display the contact data. The plots are divided into different fingers, with data for joint 1 in red, joint 2 in green, and joint 3 in blue. It is evident that the fingers behave similarly, but not identically, even if the object is symmetrical. The trajectory of the analytical prediction is more similar for the three fingers compared to the LSTM approach. Additionally, it is noticeable that once a contact is established, the joint value no longer changes for the analytical approach.

VII. Discussion

To address the first research question, we can refer to Table II. The results clearly indicate that the analytical approach cannot compete with the other two methods and is only half as accurate overall. The reason for this can be identified in Figure 9. Once a finger phalanx makes contact, the movement stops. If a contact is released, the system cannot react because the following states are calculated under

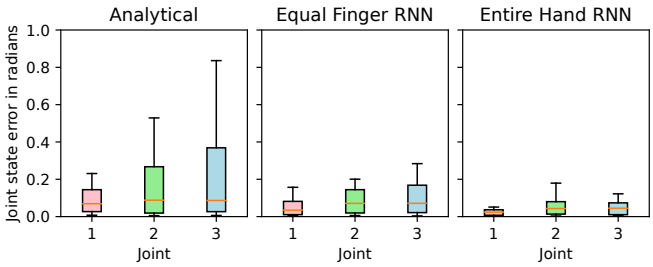

Fig. 6. The boxplots depict the error distribution of each joint for the full closing motion. On the left, from the analytical method; in the middle, from the LSTM not distinguishing between the fingers; on the right, from the LSTM method with the entire hand.

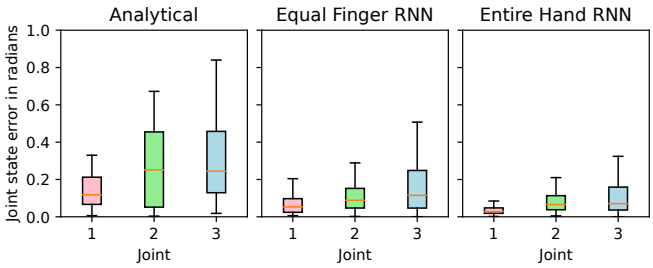

Fig. 7. The boxplots depict the error distribution of each joint for the end state of the grasp. On the left, from the analytical method; in the middle, from the LSTM not distinguishing between the fingers; on the right, from the LSTM method with the entire hand.

the wrong assumption, or more precisely, a phase would need to be reverted, which is neither provided for nor feasible in this approach. This also explains why the error increases as the fingers close further. The network of the whole hand deals with this problem better than the other network.

We compare the two deep learning approaches to address the second research question. The accuracies demonstrate that the network considering the entire hand performs better than the network treating the fingers equally. This indicates that each finger benefits from the contact information of the other two fingers and incorporates it into its own calculation. By examining the upper plots in Figure 9, it is evident that the fingers behave differently, and even though they make contact with the object, the corresponding joints still change.

Another crucial point is the deviation at the end of a grasp, which is of interest for future analyses regarding grasp evaluation and quality assessment. In Figure 8, it is evident that the analytical method becomes highly inaccurate towards the end. Additionally, Figure 7 further illustrates the error in the final states and the significant deviation from the actual state. In comparison, the estimation of the deep learning approach considering the entire hand is quite precise and can be used for further applications.

It is noticeable that the first joint is significantly more accurate, while the third joint is the least accurate (see Figure 6 and Figure 7). When moving the finger to a partially closed state, the first joint has much less range of motion compared to the other two. Additionally, due to the adaptive coupling of the finger phalanges, the joints influence each other; a change in joint 1 has a much greater impact on joint 2 and 3 than, for example, joint 3 on joint 1. This results in larger errors in joint 2 and especially joint 3.

TABLE II
AVERAGE JOINT STATE ESTIMATION ERRORS IN RADIANS

Whole closing motion	Joint 1	Joint 2	Joint 3	Overall
Analytical	0.084	0.145	0.196	0.142
RNN equal finger	0.057	0.093	0.117	0.089
RNN entire hand	**0.026**	**0.048**	**0.047**	**0.040**
End state				
Analytical	0.140	0.275	0.329	0.248
RNN equal finger	0.088	0.149	0.163	0.133
RNN entire hand	**0.045**	**0.085**	**0.107**	**0.079**

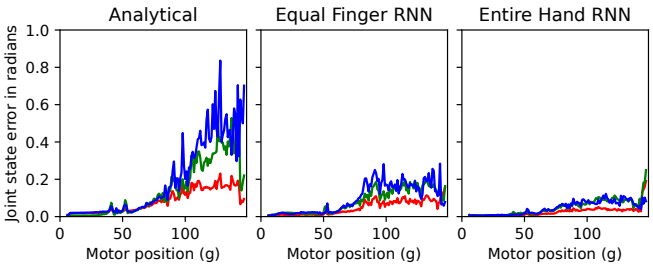

Fig. 8. The error between the predicted joint state and the measured ground truth state of a finger during a grasp. On the left, the analytical method; in the middle, the LSTM treating the fingers equally; on the right, LSTM method with the entire hand. **Red** represents the proximal phalanx (joint 1), **green** is the middle phalanx (joint 2), and **blue** is the fingertip (joint 3).

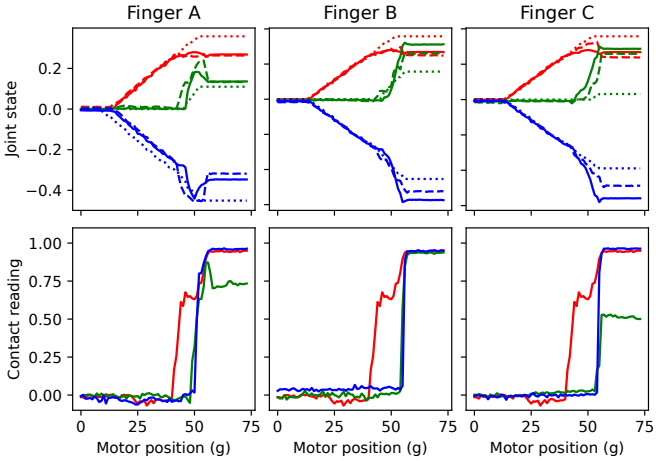

Fig. 9. The upper graphs depict the various joint state predictions during a grasp of the wooden block. The solid line represents the ground truth values, the dashed line represents the prediction of the LSTM method with the entire hand, and the dotted line represents the prediction of the analytical method. The lower graphs show the sensor readings of the respective contact sensors. **Red** represents the proximal phalanx (joint 1), **green** is the middle phalanx (joint 2), and **blue** is the fingertip (joint 3).

VIII. Conclusion

In this paper, we presented various methods for determining the joint state of the adaptive 3-finger gripper from Robotiq and compared them. The foundation of the paper was Franchi and Hauser [3] analytical approach, which reaches its limits when objects move during the grasp. A deep learning approach, considering the fingers identically similar to the analytical one, provided better results. However, it is even more effective to consider the fingers individually together as a whole to compensate for influences from other fingers and reach more robust estimation results. Overall, with our new approach, we achieved an accuracy of 0.040 radians or 2.29 degrees, with the lower joints predicted significantly more accurately than the fingertip.

Furthermore, the neural network approaches can be trained and applied on different grippers as long as ground truth data and enough tactile information is available.

Next, these results can be utilized in grasp analysis and quality assessment to plan movements even more accurately and robustly. Additionally, similar approaches could be implemented for in-hand manipulation, as discussed in [6, 9].

References

[1] L. U. Odhner and A. M. Dollar, "Dexterous Manipulation with Underactuated Elastic Hands," in *2011 IEEE International Conference on Robotics and Automation*. IEEE, 2011, pp. 5254–5260.

[2] ——, "Stable, open-loop precision manipulation with underactuated hands," *The International Journal of Robotics Research*, vol. 34, no. 11, pp. 1347–1360, 2015.

[3] G. Franchi and K. Hauser, "Technical Report: Use of Hybrid Systems to model the RobotiQ Adaptive Gripper," *Bloomington, IN*, 2014.

[4] H. Meng, K. Yang, L. Zhou, Y. Shi, S. Cai, and G. Bao, "Optimal Design of Linkage-Driven Underactuated Hand for Precise Pinching and Powerful Grasping," *IEEE Robotics and Automation Letters*, vol. 9, no. 4, pp. 3475–3482, 2024.

[5] A. Sintov, A. S. Morgan, A. Kimmel, A. M. Dollar, K. E. Bekris, and A. Boularias, "Learning a State Transition Model of an Underactuated Adaptive Hand," *IEEE Robotics and Automation Letters*, vol. 4, no. 2, pp. 1287–1294, 2019.

[6] H. Van Hoof, T. Hermans, G. Neumann, and J. Peters, "Learning Robot In-Hand Manipulation with Tactile Features," in *2015 IEEE-RAS 15th International Conference on Humanoid Robots (Humanoids)*. IEEE, 2015, pp. 121–127.

[7] W. M. Mohammed, M. Nejman, F. Castaño, J. L. M. Lastra, S. Strzelczak, and A. Villalonga, "Training an Under-actuated Gripper for Grasping Shallow Objects Using Reinforcement Learning," in *2020 IEEE Conference on Industrial Cyberphysical Systems (ICPS)*, vol. 1. IEEE, 2020, pp. 493–498.

[8] M. Liu, Z. Zhao, W. Zhang, and L. Hao, "Reinforcement learning control of a humanoid robotic hand actuated by shape memory alloy," *Proceedings of the Institution of Mechanical Engineers, Part C: Journal of Mechanical Engineering Science*, vol. 235, no. 21, pp. 5736–5744, 2021.

[9] O. Azulay, I. Ben-David, and A. Sintov, "Learning Haptic-Based Object Pose Estimation for In-Hand Manipulation Control With Underactuated Robotic Hands," *IEEE Transactions on Haptics*, vol. 16, no. 1, pp. 73–85, 2022.

[10] T. Matsuno, Z. Wang, and S. Hirai, "Grasping state estimation of printable soft gripper using electro-conductive yarn," *Robotics and Biomimetics*, vol. 4, no. 1, pp. 1–11, 2017.

[11] T. Li, L. Qiu, and H. Ren, "Distributed Curvature Sensing and Shape Reconstruction for Soft Manipulators With Irregular Cross Sections Based on Parallel Dual-FBG Arrays," *IEEE/ASME Transactions on Mechatronics*, vol. 25, no. 1, pp. 406–417, 2019.

[12] V. A. Ho and S. Hirai, "Measuring McKibben Actuator Shrinkage Using Fiber Sensor," in *2015 24th IEEE International Symposium on Robot and Human Interactive Communication (RO-MAN)*. IEEE, 2015, pp. 628–633.

[13] L. Yan, J. Hao, Z. Zhang, R. Liu, H. Yang, and C. Shi, "Curvature Estimation of Soft Grippers Based on a Novel High-Stretchable Strain Sensor with Worm-Surface-like Microstructures," *IEEE Sensors Journal*, 2023.

[14] T. Laliberté and C. M. Gosselin, "Simulation and design of underactuated mechanical hands," *Mechanism and machine theory*, vol. 33, no. 1-2, pp. 39–57, 1998.

[15] A. Rocchi, B. Ames, Z. Li, and K. Hauser, "Stable Simulation of Underactuated Compliant Hands," in *2016 IEEE International Conference on Robotics and Automation (ICRA)*, 2016, pp. 4938–4944.

[16] G. M. Achilli, S. Logozzo, M. C. Valigi, and M. Malvezzi, "Preliminary Study on Multibody Modeling and Simulation of an Underactuated Gripper With Differential Transmission," in *International Design Engineering Technical Conferences and Computers and Information in Engineering Conference*, vol. 85468. American Society of Mechanical Engineers, 2021, p. V009T09A005.

[17] A. S. Sadun, J. Jalani, and F. Jamil, "Grasping Analysis for a 3-Finger Adaptive Robot Gripper," in *2016 2nd IEEE International Symposium on Robotics and Manufacturing Automation (ROMA)*. IEEE, 2016, pp. 1–6.

[18] N. Fiedler, P. Ruppel, Y. Jonetzko, N. Hendrich, and J. Zhang, "Low-cost fabrication of flexible tactile sensor arrays," *HardwareX*, vol. 12, p. e00372, 2022.

[19] J. Wang and E. Olson, "Apriltag 2: Efficient and robust fiducial detection," in *2016 IEEE/RSJ International Conference on Intelligent Robots and Systems (IROS)*. IEEE, 2016, pp. 4193–4198.

[20] H. Sak, A. W. Senior, and F. Beaufays, "Long Short-Term Memory Recurrent Neural Network Architectures for Large Scale Acoustic Modeling," *Interspeech 2014*, 2014.

[21] B. Calli, A. Walsman, A. Singh, S. Srinivasa, P. Abbeel, and A. M. Dollar, "Benchmarking in Manipulation Research: Using the Yale-CMU-Berkeley Object and Model Set," *IEEE Robotics & Automation Magazine*, vol. 22, no. 3, pp. 36–52, 2015.